BRAZILIAN JOURNAL OF FOOD TECHNOLOGY

ISSN 1981-6723
Online version

ORIGINAL ARTICLE

Continuously monitored lactose crystallization in a vibrated bed

Cristalização de lactose em leito vibrado com monitoramento contínuo

Gustavo Araújo Teixeira[1]*, Fabio Ferreira Batista[2], Ricardo Amâncio Malagoni[3], José Roberto Delalibera Finzer[4]

[1]Universidade Federal do Triângulo Mineiro, Departamento de Engenharia de Alimentos, Uberaba/MG - Brasil
[2]Mettler-Toledo AutoChem, Inc. - United States
[3]Universidade Federal de Uberlândia, Faculdade de Engenharia Química, Uberlândia/MG- Brasil
[4] Universidade de Uberaba, Faculdade de Engenharia Química, Uberaba/MG - Brasil

***Corresponding author:** Gustavo Araújo Teixeira, Universidade Federal do Triângulo Mineiro, Departamento de Engenharia de Alimentos, Avenida Dr. Randolfo Borges Júnior, 1250, Universidade, CEP: 38064-200, Uberaba/MG - Brasil, e-mail: gustavo.teixeira@uftm.edu.br

Cite as: Teixeira, G. A., Batista, F. F., Malagoni, R. A. & Finzer, J. R. D. (2019). Continuously monitored lactose crystallization in a vibrated bed. *Brazilian Journal of Food Technology*, *22*, e2018275. https://doi.org/10.1590/1981-6723.27518

Abstract

The aim of this work was to evaluate the crystal size distribution (CSD) and microscopy of the crystalline phase in isothermal lactose crystallization, using a high seeding concentration (dense phase). In-line monitoring was carried out using Focused Beam Reflectance Measurement (FBRM) and Particle Vision Measurement (PVM) probes in a stainless steel trunk-conical shaped jacketed crystallizer. The vibratory shaking system consisted of two perforated discs coupled to a movable axle. A conventional crystallization unit, with a three-blade propeller attached to a stainless steel shaft, was used for comparison. Concentrated cheese whey, purified with an organic coagulant, and commercial lactose solutions were used. Crystallization was improved in the high-purity solutions. Microparticles and/or aggregates appeared before seeding, mainly in the purified cheese whey solution, in which there are impurities. Secondary nucleation was present in both the vibratory agitation and conventional rotary agitation systems, being intensified by increases in agitation. Crystallization in a vibratory system should be carried out with a vibration frequency of 250 rpm, since an increase to 400 rpm reduced the amount of larger crystals.

Keywords: Vibrated bed; Lactose; Crystallization; In situ monitoring; In line monitoring; Isothermal.

Resumo

O estudo visa avaliar a distribuição de tamanho cristalino e a microscopia da fase cristalina na cristalização isotérmica de lactose, usando alta concentração de sementes (fase densa). O monitoramento *in-line* foi realizado utilizando as sondas de medição de reflexão de feixe focalizado (FBRM) e de medição de visão de partículas (PVM), um cristalizador de aço inoxidável encamisado, em formato tronco-cônico. O sistema de agitação vibratório foi composto por dois discos perfurados, acoplados a um eixo móvel. Uma unidade de cristalização convencional, com três pás do tipo hélice conectadas a um eixo de aço inoxidável, foi utilizada como comparação. Utilizou-se soro de queijo concentrado, purificado com um coagulante orgânico, e soluções de lactose comercial. O rendimento da

cristalização foi aumentado em soluções de alta pureza. Houve presença de aglomerados e/ou agregados antes da semeadura, principalmente nas soluções de soro purificado, nas quais há impurezas. A nucleação secundária esteve presente nos experimentos, tanto no sistema com agitação por vibração quanto no sistema de agitação convencional por rotação, sendo intensificada pelo aumento da agitação. A cristalização em leito vibrado deve ser realizada com uma frequência de vibração de 250 rpm, porque um incremento a 400 rpm reduz o número de cristais maiores.

Palavras-chave: Leito vibrado; Lactose; Cristalização; Monitoramento *in situ*; Monitoramento *in-line*; Isotérmico.

1 Introduction

The manufacture of lactose (mostly α-lactose monohydrate) from whey involves purification (liming, heat treatment and filtration), whey concentration, refiltration, crystallization and centrifugation. In general, about 50% lactose recovery is achieved, and the remaining mother liquor is used to produce lactose whey powder. This process has been proven to be commercially efficient on a large scale (Zadow, 1984).

Crystallization is considered the most important concentration step in the manufacture of lactose from whey; but the crystallization process is far from optimal on an industrial scale. Filling the tank takes about 6 h and is followed by gradual cooling and crystallization, which takes from 14 to18 h, such that the whole crystallization process takes from 20 to 24 h (Shi et al., 2006). The crystallization step is usually carried out in a large, cold, stirred crystallizer and as the solution gradually cools the supersaturation level increases, and lactose crystals develop. Crystal growth is typically accompanied by secondary nucleation, so that the final product contains many small crystals, as shown in Figure 1. The resulting crystal size distribution negatively influences the subsequent processes (filtration, washing, drying) and results in a low-quality product, large product losses and low yields (Wong et al., 2012).

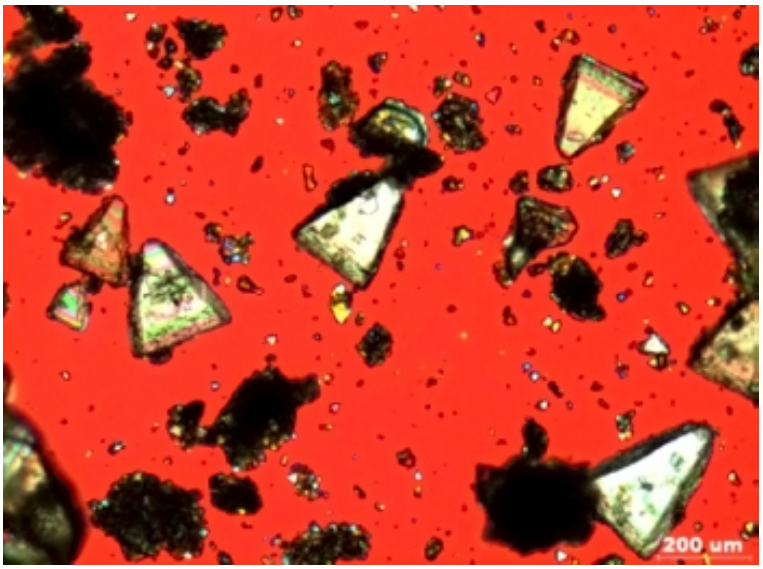

Figure 1. Crystalline lactose particles from industrial crystallizers (Wong et al., 2012).

To overcome this problem, the crystallization process can be improved by operating under conditions that promote growth and minimize secondary nucleation, leading to the production of larger crystals with a narrower crystal size distribution (Wong et al., 2011). The rate at which crystallization occurs depends on many variables, including the crystal surface available (which depends on the seed sizes), supersaturation level, temperature, the presence of salts and the solution viscosity (Caric, 1994).

According to Lifran et al. (2007), lactose crystals tend to incorporate protein molecules, salts and even biopolymers during crystallization, which lowers the final product purity and inhibits crystallization, and the concentration of impurities influences the size and shape of the crystals. Crystal growth can be interrupted by impurities incorporated in the crystal structure or by their adsorption onto the crystal surface. Impurities can also modify the structure, size and habits of the crystalline product. Small concentrations of specific impurities in supersaturated solutions can enable nucleation, change the growth and influence aggregation and the morphology of the crystals during growth (Markande et al., 2012). Therefore, for effective crystallization, interferents present in the whey such as water-soluble proteins, lactose and varying amounts of minerals, especially calcium, phosphate and various monovalent ions, should be removed. The whey composition is highly variable (De Wit, 2001; Gernigon et al., 2009), so it is difficult to act on all the contaminants during process optimization.

The stirring of the whey favours the development of lactose crystals, when small seeds are brought into contact with a supersaturated whey solution (Early, 1998). In addition, constant stirring breaks up larger crystals, avoids the deposition of crystals at the bottom of the tank and helps maintain the viscosity (Walstra, 2003). Without stirring, the whey concentrate becomes very viscous due to a high degree of primary nucleation, which decreases the rate of lactose crystallization (Modler & Lefkovitch, 1986; Jayaprakasha et al., 1995).

In general, the use of an impeller in a crystallizer results in smaller and more uniform crystals (Mullin, 1988). However, it also induces secondary nucleation and the chord length shows a tendency to increase with reduced stirring speeds. Particle breakage and aggregation can induce the deviation of chord length from linearity, in addition to creating large numbers of small particles by secondary nucleation and growth (Kutluay et al., 2017).

Using a vibration system composed of a disc immersed in a solution which caused vertical vibrations of small amplitude, Fedyushkin et al. (2005) evaluated the influence of vibration in the crystallization system. The results were obtained using a laser shadow-graphic method and showed that a controlled vibration decreases the thickness of the boundary layers of the solid–liquid interface, which means that it can positively modify the temperature and concentration gradients and the crystal growth rate.

The main milk carbohydrate is lactose ($C_{12}H_{22}O_{11}$), a disaccharide consisting of glucose and galactose linked by a (1,4) glycosidic bond, and two isomers exist naturally: α-lactose and β-lactose (Figure 2).

In a batch process, where the α-lactose crystallizes from an aqueous solution, the concentration of α-lactose present in solution decreases over time, which causes an increase in the ratio between the two forms in solution.

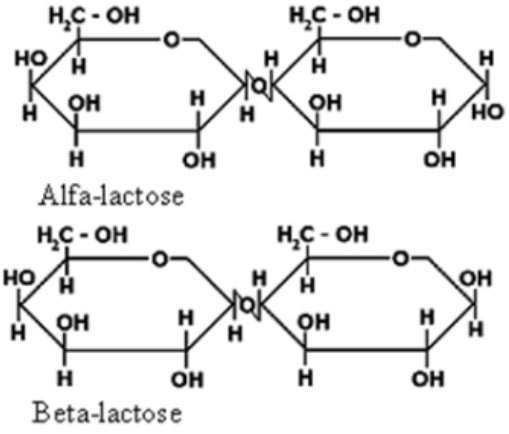

Figure 2. Structural configurations of the lactose isomers.

The solubility of the lactose isomers in water is low in comparison with other disaccharides, but the effect of temperature on their solubility is more pronounced. At equilibrium, the ratio between the isomers, α/β = 1/1.6, and complete solubility of the α form is 180 g L^{-1} at 20 °C. Despite the greater proportion of the β form, the α form is that which crystallizes in foods, due to its lower solubility. During the crystallization of α-lactose, β-lactose remains in solution and is slowly converted into the α form by mutarotation, until the solution becomes saturated. At temperatures below 93.5 °C, it is the α-lactose which crystallizes, while above this temperature, β-lactose crystallizes. The isomer α-lactose crystallizes as a monohydrate and β-lactose as anhydrous crystals (Finzer & Malagoni, 2016).

The limiting step in the two-step mechanism of mutarotation has been studied by several authors and proven to be dependent upon various experimental conditions such as pH, the level of seeding crystals and the surface area. It has been clearly established that mutarotation exerts a crucial role in the lactose crystallization rate when there is a large crystalline surface area (Twieg & Nickerson, 1968).

The aim of this study was to evaluate monohydrate lactose crystallization from commercial and organically purified whey matter solutions, with in situ and in line monitoring, the crystal size distribution and microscopy (nucleation/aggregation), using conventional batch and vibrated units.

2 Materials and methods

2.1 Purification of cheese whey

The organic coagulant Tanfloc SG® (Tannate quaternary ammonium), a biodegradable cationic polymer that does not change the pH of the solution to be treated, supplied by the company TANAC SA, was used to purify the cheese whey.

The cheese whey was provided by the company CALU (Agricultural Cooperative LTDA Uberlândia, MG).

Initially, the Tanfloc coagulant was added at different rates to natural cheese whey samples, each with a volume of 1.0×10^{-3} m^3, in borosilicate vessels. The resulting mixture was then stirred using a cylindrical magnetic stirrer (4.0×10^{-2} m; Tecnal, TE-085) for 0.17 h (900 to 1000 rpm), followed by milder stirring (400 to 500 rpm) for 0.083 h.

The samples treated with Tanfloc were transferred to separating funnels, and allowed to rest for 2 h, forming three phases: an upper solid phase with a white colour, an intermediate liquid phase, and another solid white phase at the bottom. The top and bottom solid fractions were discarded, and the solution subjected to centrifugation using a Beckman Coulter J26 centrifuge (25.65-cm radius), with a frequency of 5000 rpm and duration of 0.083 h.

After centrifugation, the samples were filtered using Qualy quantitative filter paper with a pore size of 14.0×10^{-6} m and diameter of 12.5×10^{-2} m, using a Büchner funnel (Chiarotti Mauá, 03-90), with a vacuum of 200 mmHg.

The Gerber method was selected to quantify the fat in the cheese whey.

The lactose content of the cheese whey solutions was determined using the dinitrosalicylic acid (DNS) method with a spectrophotometer (PG Instruments, T60 UV – Visible Spectrophotometer). The standard curve of absorbance versus lactose concentration was prepared using solutions with known concentrations of absolute lactose (Proquímios, purity > 99.5%), in triplicate.

The protein concentrations in the fresh and purified cheese wheys were quantified using the Lowry method. The standard curve of absorbance versus protein concentration was prepared using solutions with known concentrations of bovine albumin (UBS brand, purity > 98%).

The fat, protein and lactose concentrations indicated that the treatment of the sample with 2×10^{-6} m^3 Tanfloc L of whey^{-1} was the most efficient treatment, giving final concentrations of 0.05% fat and 4.126 ± 0.706 g L^{-1} protein (90% fat and 40.3% protein removal).

2.2 Concentration of the lactose in the cheese whey

The purified whey was subjected to a concentration process to obtain a saturated solution. Before the concentration process, the lactose content was determined by the DNS method, in triplicate.

The amount of whey to be concentrated was calculated from the ratio between the lactose concentration in the initial solution of purified whey and the desired final concentration of lactose in the solution (C = 85.16 kg of lactose 100 kg of water^{-1}), according to the experimental design of Teixeira (2014).

A rotoevaporator with a vacuum pump (Quimis model 355 B2) was used. Portions of 0.50×10^{-3} m^3 of cheese whey were submitted to evaporation in batches. The rotoevaporator was operated under a vacuum of 200 mmHg at a temperature of 85 °C and frequency agitation of 21 rpm. Under these conditions, the rate of evaporation was 7.5×10^{-3} L of water min^{-1}.

The pressure was not fixed since there was intense bubble formation during the concentration process, especially at lower pressures.

At the end of the concentration stage, the concentrated undersaturated solution had a predetermined volume of 280×10^{-3} L, and the sample was maintained at 85 °C.

The concentrated solution was filtered and kept hermetically stored until the moment of the crystallization operation, when it then had to be heated again to a temperature 10 °C above the lactose solution saturation temperature (73.5 °C) for a period of approximately 1.0 h.

2.3 Crystallization trials

The crystallization procedure was carried out with the insertion of a concentrated solution (C = 85.16 kg of lactose/ 100 kg of water^{-1}) in a crystallizer at a saturation temperature of 73.5 °C, maintained by a thermostatic water bath. After a 5-min interval, the solution was cooled to 50.0 °C, the operating temperature, in a period of approximately 0.5 h.

During the cooling process, the crystallizer was set to the predicted frequency, determined in a previous operational optimization (Teixeira, 2014), and measured using a digital tachometer (Shimpo, DT 205B). The value of the vibration frequency was obtained from Equations 1 and 2 (Pakowski et al., 1984).

$$\omega_{ex} = r\frac{2\pi}{60} \tag{1}$$

$$\Gamma = \frac{A_{ex}\omega_{ex}^2}{g} \tag{2}$$

where ω_{ex} is the angular vibration frequency in 1 s^{-1}, r is the eccentric agitation velocity in rotations per minute (rpm), A_{ex} is the range of the exciter agent in m, g is the acceleration of gravity in m s^{-2}, and Γ is the dimensionless vibration number, used to quantify the vibration energy imposed on the system and to characterize the vibrofluidized bed.

Once the operating temperature had been reached, the pre-determined amount of seed of 1.78×10^{-1} kg L^{-1} of solution was added to the crystallizer. The Sauter mean diameter (SMD) of the seeds was 5.612×10^{-6} m. This dense phase (high seed population) was used to approximate industrial seeding conditions.

Successive 3.0×10^{-3} L slurry samples were taken at 0.5-h intervals after seeding, up to the end of the crystallization period, to determine the average crystal size during the crystallization step. The first sample

was taken at 0.334 h, and to monitor the lactose concentration in solution during crystallization, 1.0×10^{-3} L samples of the mother liquor were also taken from the crystallizer at the same sampling times.

To quantify the crystal mass, the samples were vacuum filtered (Quimis model 355 B2) using a Kitasato borosilicate glass funnel coupled to a 600 Tyler screen. The filtrate was immediately washed with ethyl alcohol PA (Kinetics – 99.5%) and finally dried at 60 °C for 24 h in an oven (Medicate, MD 1.3). The crystals obtained at the second sampling point were washed with 75° GL ethyl alcohol and subsequently with ethyl alcohol PA. Each dried sample of filtrate was weighed on a balance (Gehaka BG200, with a resolution of 10^{-4} g). The particle size was determined using a Malvern Mastersizer equipment.

Tests were also carried out with solutions prepared with commercial lactose, seeding under similar operational conditions.

During some experiments, some changes (seeding charge or stirring speed) were made to the process conditions, in order to evaluate the behaviour of the monitored responses.

2.4 Seed production

The saturated solution prepared at 57 °C was cooled to 7 °C at a rate of 0.139 °C min^{-1} (6 h) with magnetic stirring at approximately 300 rpm, remaining at this temperature for 24 h.

The solution used was commercial α-lactose monohydrate (Granulac 200, Meggle) dissolved in distilled water, the concentration being calculated using the solubility equation (Teixeira, 2014). Subsequently, this solution was placed in contact with water in a thermostatic bath (Tecnal, TE-184) at a temperature of 57 °C until the solution became homogeneous. The solution was subsequently poured into a 0.5×10^{-3} m^3 conical flask, stirred at approximately 700 rpm with a magnetic stirrer (Tecnal, TE-085), and then inserted into the refrigerated compartment at a temperature of 7 °C to start the cooling process. The temperature of the suspension was monitored throughout the whole period using a FullGage Controls TIC17RTG calibrated thermocouple.

After 24 h, the slurry was vacuum filtered using a 0.5×10^{-3} m^3 Kitasato borosilicate flask, a Büchner funnel and quantitative filter paper with an area of 12.5×10^{-2} m and porosity of 0.8 μm, connected to a Quimis 355 B2 vacuum pump.

This procedure allowed for crystal formation by primary, homogeneous or heterogeneous nucleation, due to the high degree of supersaturation and, probably, by secondary nucleation caused by friction between the crystals formed and the fixed/mobile parts (magnetic bar) of the crystallizer, with subsequent growth.

The seed crystals were dried for 48 h at 60 °C in an oven (Medicate, model MD 1.3).They were then weighed and 0.50×10^{-1} kg portions applied to a sieve shaker (Retsch, AS 200) to select the seed range of interest. The crystals selected were those retained between the 200 and 500 Tyler sieves, with the intermediate 250, 325 and 400 Tyler sieves (which divided the sample mass) maintained at selected intervals.

The average size of the seed crystals (SMD) was then quantified using the Malvern Mastersizer equipment.

2.5 Experimental apparatus

Lactose crystallization was effected using a stainless steel trunk-conical jacketed crystallizer, with the conical section at an angle of 65° to the horizon, at a temperature of 50.0 °C (Shi et al., 2006) controlled by a thermostatic bath (TECNAL, TE – 184). Figure 3 shows the configuration of the crystallizer.

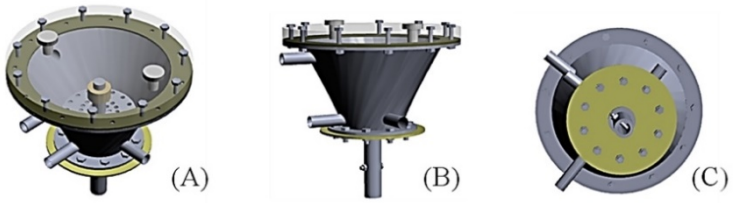

Figure 3. Schematic views of the vibrated bed crystallizer: (A) acrylic cover with inspection holes for seed addition and sample removal; (B) side access points for insertion of the thermocouple and temperature control of the crystallizer; (C) synthetic rubber polymeric membrane that holds the processed material in the vessel and imparts momentum to the suspension.

The solution was mixed using two perforated 1.17×10^{-3} m-thick discs with diameters of 60×10^{-3} and 80×10^{-3} m, fixed to the oscillating shaft centre. Metal rings assured the spacing between the lower disc and the insulating membrane between the two discs, and between the upper disc and a stop, measuring 1.5×10^{-2}, 2.0×10^{-3} and 2.0×10^{-3} m, respectively. The larger disc was made with three rows of orifices, totalling 40 holes, and the disc with the smaller diameter had two rows containing eight orifices. The diameter of the orifices was 5×10^{-3} m. Figure 4 presents the shaking system of the crystallizer.

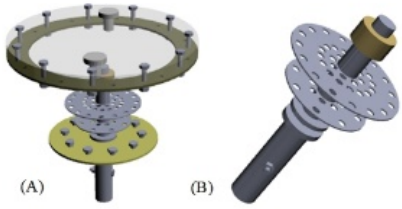

Figure 4. Schematic diagram of agitation system inside the crystallizer.

Two sampling points were selected. The first was located between the two internal stirring discs, which corresponds to the central portion of the crystallizer, at a distance of 6.53×10^{-3} m from the upper disc. The second one was placed at the bottom of the crystallizer, next to the rubber bottom seal (see Figure 4).

FBRM® (Focused Beam Reflectance Measurement) was used for the in-process measurement of the particles. A chord length distribution (CLD), sensitive to particle size and count, was reported in real time without the need for sampling. PVM® (Particle Vision Measurement) was used to view and save real-time microscope-quality images of the crystals as they naturally formed during the process – at full process concentration.

The FBRM® and PVM® probes were inserted through the top cover, which was perforated according to the characteristic dimension of the probes coupled in sealing polymer stoppers, which ensured sealing of the bed. To insert the probes into the crystallization slurry, holes were made in the vibrating discs based on the probe dimensions. The FBRM® and PVM® probes were positioned at distances of 94.9×10^{-3} and 95.2×10^{-3} m, respectively, from the top cover of the crystallizer, located in the central portion of the bed slurry.

Figure 5 shows the schematic diagram of the crystallizer with the probes already inserted.

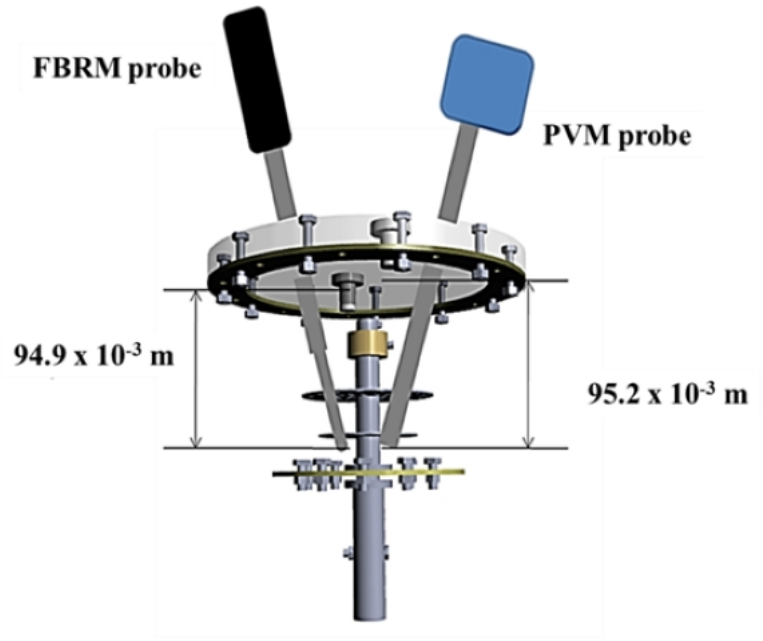

Figure 5. Schematic diagram of the probes in the crystallizer.

The crystallization trials were also carried out with an Easymax® conventional drive system, which is an electrically heated crystallizer working at a controlled temperature, with 150 mL capacity crystallization vessels, stirring at 30 to 1200 rpm using a powered mechanical stirrer with blades, internal temperature control, and a support system for the FBRM® and PVM® probes. Figure 6 illustrates the conventional crystallization unit used.

Figure 6. Easymax® system with FBRM® and PVM® probes.

In the conventional unit, the tests were carried out with purified whey concentrate and with commercial prepared lactose solutions, maintaining the same process conditions.

3 Results and discussion

Lactose crystallization tests, with in situ monitoring using the FBRM and PVM technologies, were carried out with solutions prepared with commercial lactose and purified concentrated milk whey solutions (treated with Tanfloc).

3.1 Crystallization with a commercial lactose solution in a dense phase

The solution used in these experiments (both units) was prepared with commercial lactose; the saturation concentration would result in a supersaturation level (1.88) corresponding to the optimal value obtained in the CCD with seeding for the operating temperature of 50.0 °C (Teixeira, 2014); see Equation 3.

$$S = \frac{\bar{X}}{\bar{X}^{sat}} \tag{3}$$

Figure 7 shows the particle count and chord length recorded by the FBRM equipment during the entire lactose crystallization process in the conventional unit. The PVM images are reported together.

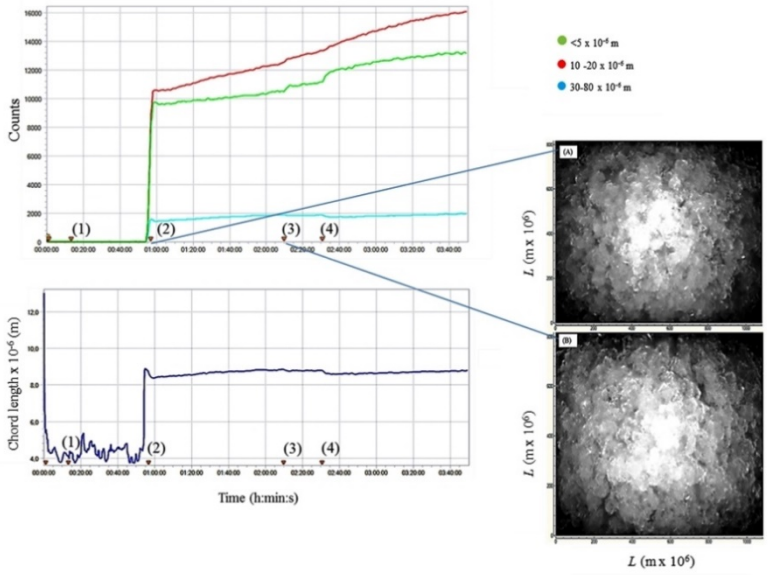

Figure 7. Particle count and chord length as a function of crystallization time for the ranges < 5.0 × 10^{-6}, 10 to 20 × 10^{-6} and 30 to 80 × 10^{-6} m. Point (1): insertion of the solution into the crystallizer and adjustment of rotation to 250 rpm; Point (2): seeding; Point (3): stirring velocity adjusted to 500 rpm; Point (4): stirring velocity adjusted to 800 rpm.

The presence of large numbers of crystals with chord lengths shorter than 20 × 10^{-6} m (representing more than 93% of the crystal population) was quantified after seed addition to the crystallizer (2), as well as a significant increase in the number of crystals during the crystallization process.

A small and slow increase in chord length occurred, mainly due to the large amount of crystals used in seeding (2).

The increase in the number of fines (crystals smaller than 5 × 10^{-6} m) was probably related to secondary nucleation phenomena, caused by friction between the crystals and components of the crystallizer and crystal−crystal interactions. No ultimate distinction between secondary nucleation and growth can be made in order to explain the formation of smaller crystals when large size variations in seed particles are used (Linga, 2017). The changes in agitation velocity caused an increase in the number of particles smaller than 20 × 10^{-6} m.

Dense phase operation provides a large number of crystals already in the bed, and hence the distinction of crystals in the images was impossible. This was noted after seeding (A). In the (B) capture, the distinction becomes even more difficult, precisely because of the increase in the number of particles, which was approximately 20%.

Vibrational crystallization was carried out under the same operational conditions as conventional crystallization ($\Gamma = 0.54$; $A_{ex} = 4.855 \times 10^{-3}$ m).

Figure 8 shows the count as a function of time as registered by the FBRM equipment throughout the stage in the vibration unit.

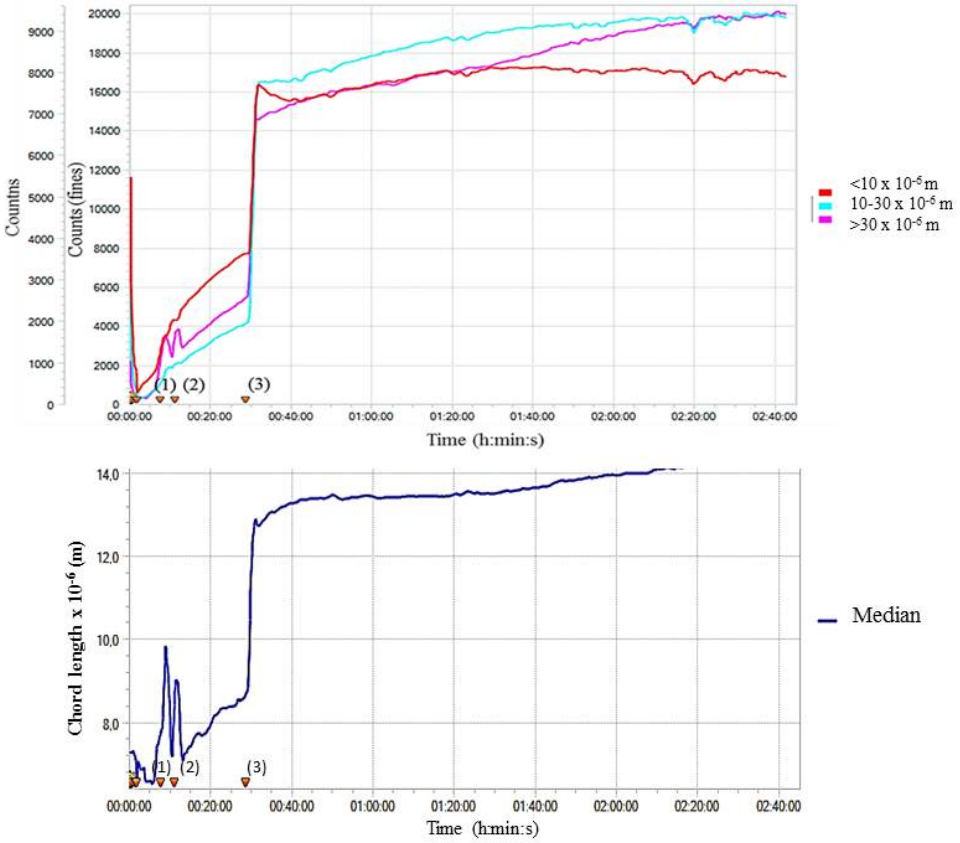

Figure 8. Particle count and chord length as a function of crystallization time for the ranges < 10.0×10^{-6} (fines), 10 to 30×10^{-6} (fines) and > 30×10^{-6} m. Point (1): insertion of the solution into the crystallizer, stirring velocity adjustment; Point (2): cooling start; Point (3): seeding.

During the process of cooling the solution to the operational temperature (unseeded bath), Figure 8 indicates an increased presence of microparticles in the solution (after point 2), probably related to the increase in supersaturation, causing primary nucleation (Narducci et al., 2011). This phenomenon was not observed in the conventional unit, indicating inefficient stirring before seeding in the vibrating unit. However, there was significant growth of the crystal population 1 h and 20 min after the seeding operation, at which time stagnation in the number of particles < 10.0×10^{-6} m and a significant increase in particles > 30×10^{-6} and 10 to 30×10^{-6} m occurred. The latter size range showed a slight increase after a period of 2 h and 30 min, enhanced performance in relation to the conventional unit, probably due to the decrease in secondary nucleation phenomena in the vibration unit. The median data represent an increase in the average crystal size throughout the crystallization step.

The crystal images obtained during the process of cooling the solution to the operational temperature indicated an increased presence of microparticles in solution, probably related to primary nucleation. Figure 9 shows the images during this period. After seeding, the images were not well resolved due to the large number of particles in solution (dense phase), which restricted the analysis of the process images.

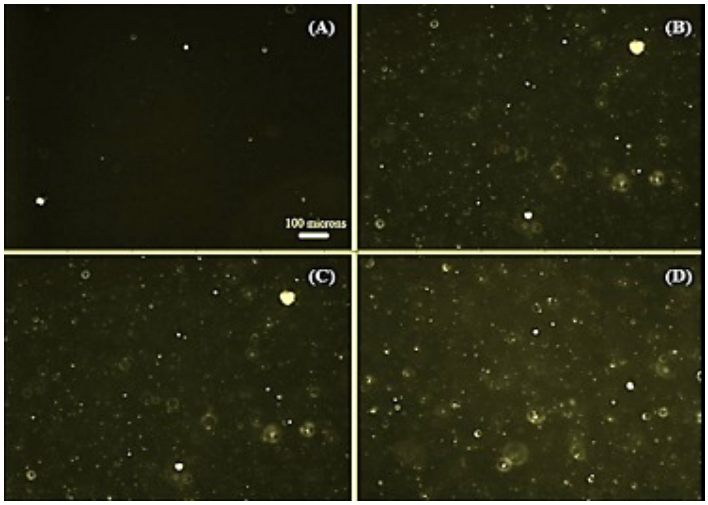

Figure 9. Images obtained during cooling of the solution to the operational temperature, in the vibration unit. (A) 2 min; (B) 9 min; (C) 19 min; (D) 28 min.

The procedures enabled a comparison between the conventional and vibration crystallizers: 1) an increase in the number of particles smaller than 5 µm and up to 20 µm in the conventional apparatus was significant. This behaviour was not observed in the vibrated system, due to a milder mixing action with the vibrational technique; 2) the increase in the number of particles between 30 and 80 µm was small in the conventional crystallizer, but in the vibrated system, the number of particles in this size range increased by over 30% after seeding. This indicates that comparing the two techniques used, the vibrated system allows for better results in terms of particle uniformity and size distribution.

3.2 Crystallization with concentrated whey solution in the dense phase

The solution used was prepared by concentrating purified cheese whey with Tanfloc until the mass concentration indicated was 46% (lactose/solution), thereby achieving the desired concentration at a degree of supersaturation of 1.88 for an operational temperature of 50 °C.

Figure 10 shows the number of particles in the different size ranges before seeding in the vibrational process, and the chord lengths.

Before seeding, microparticles were present as from the beginning of the cooling process, possibly consisting of impurities present in the whey concentrate, such as salts, fats and protein, which may also have promoted primary nucleation of the lactose available in the supersaturated solution at the beginning of the process. The unusually accelerated rate of crystal growth at the start of batch crystallization may have been due to repair of the crystal surface, poisoning from unidentified impurities or a roughening transition (Srisa-Nga et al., 2006).

The variation in the number of larger particles after seeding (37 min) was insignificant up to about 110 min, and the count for particles in the 30 to 80 × 10^{-6} m range remained practically stable, as shown in Figure 10.

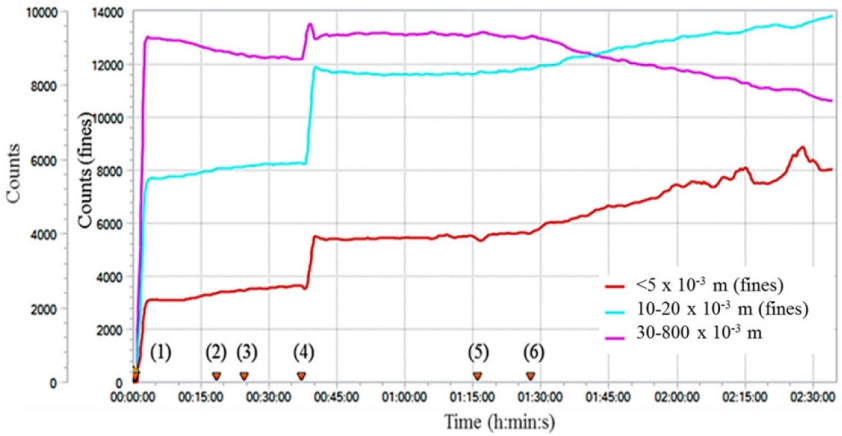

Figure 10. Particle counts in the concentrated whey crystallized using vibration. Point (1): insertion of the solution into the crystallizer, adjustment of the stirring velocity (250 rpm) and beginning of the cooling step (temperature of 73.5 °C); Point (2): temperature of 55.9 °C; Point (3): temperature of 51.3 °C; Point (4): seeding with dimensionless vibration number of Γ = 0.54 (250 rpm and 50 °C temperature); Point (5): changing of the eccentric stirring velocity to 400 rpm; Point (6): changing of the eccentric stirring velocity to 500 rpm.

Increases in the vibration frequency induced specific changes in the number of particles. There was a large increase in the number of particles in the ranges of $< 5.0 \times 10^{-6}$ and 10 to 20×10^{-6} m and a decrease in the number of particles in the range of 30 to 80×10^{-6} m, caused by increased circulation of the suspension, with secondary nucleation and breakage (Shin & Kim, 2002).

Figure 11 shows the particle size distribution before seeding (37 min), with little change up to a processing time of 35 min, probably indicating the presence of impurities in the solution, with possible primary nucleation during the period. The run time of 39 min immediately after the seeding step, was the basis for the analysis of the following operation, with an enlargement of the distribution curve (times 56 and 72 min) and an increase in the number of small particles after increasing the stirring frequency (120 min).

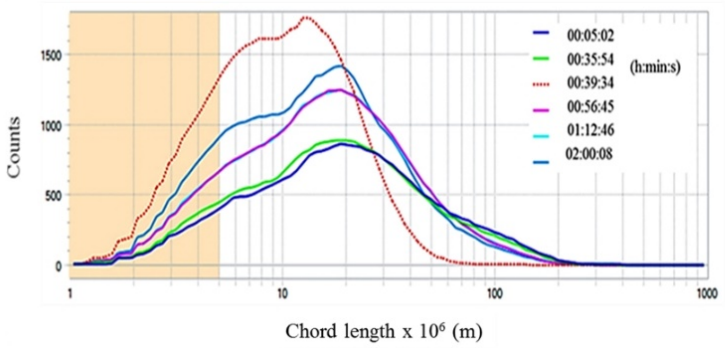

Figure 11. Crystal size distribution in the concentrated whey crystallized using vibration.

Figure 12 shows the images for the period when the solution was inserted into the vibrational crystallizer and during the cooling phase.

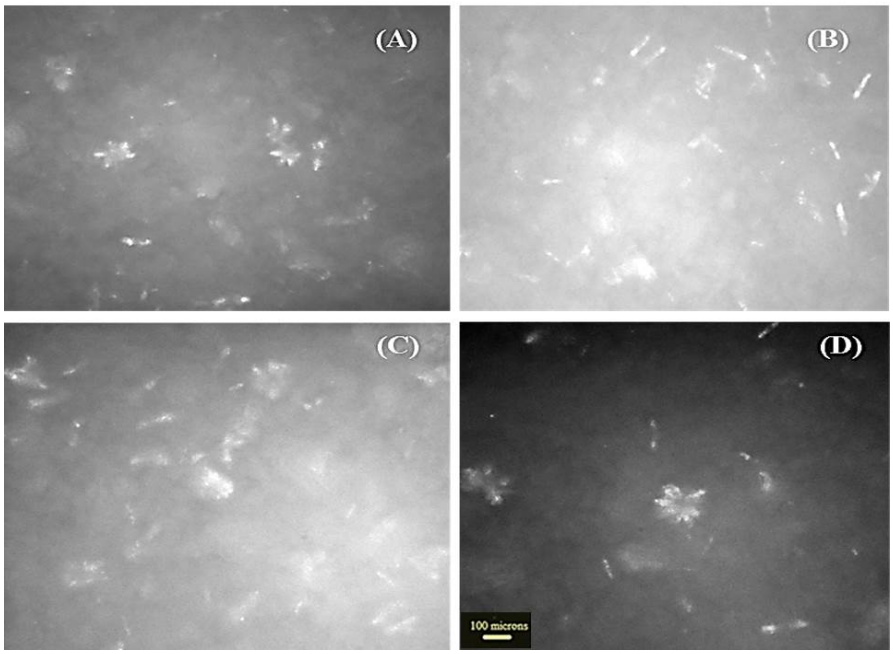

Figure 12. Images of crystals produced by vibrational crystallization: (A) insertion of the solution into the crystallizer – saturated solution; (B) 2 min after insertion of the solution, saturated solution; (C) cooling step at $T = 55.9$ °C; (D) 20 min after seeding, $T = 50.0$ °C.

Figure 12 shows that particles were already present in the solution at the beginning (A). After the start of the cooling stage, needle-like particles emerged, characteristic of lactose crystallization at a high degree of supersaturation and low degree of agitation (Parimaladevi & Srinivasan, 2014). These crystals were possibly onohydrated lactose, formed by interfering action such as nucleation centres. During the cooling procedure, stable nuclei formed until the system reached the operational temperature (50.0 °C).

Figure 13 shows the images obtained after seeding in the vibrated lactose crystallization experiments.

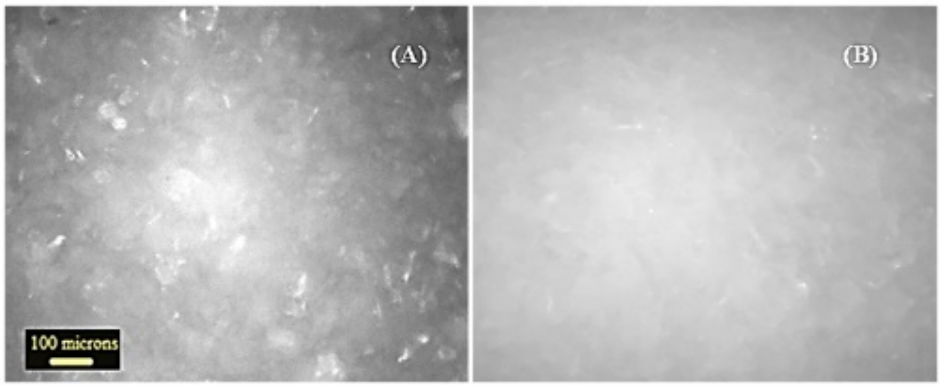

Figure 13. Images produced by vibrational crystallization: (A) insertion of the seeds into the crystallizer – captured at seeding; (B) 46 min after seeding, 400 rpm eccentric agitation velocity.

After the seeding procedure (A), resulting in the production of a dense phase, the presence of acicular and pyramidal crystals in suspension was noted. With the increase in eccentric agitation velocity to 400 rpm (B), crystal breakage occurred, thereby providing the secondary nucleation phenomenon.

In order to better monitor the crystal habits, nucleation and other process conditions during the crystallization step, a trial was carried out with 10% of the seeding proportion used in the dense phase

experiments in the conventional crystallizer, fixed at 0.01786 kg of seed L solution^{-1} and hence operating in the dilute phase. Figure 14 shows the number of particles in the different size ranges in the dilute phase test.

After the preliminary cooling, the presence of contaminants and the occurrence of primary nucleation were already apparent. After seeding, there was an increase in the number of particles, which became even more significant on increasing agitation in the bed, except for particles between 30 and 80 × 10^{-6} m which showed a decrease in numbers.

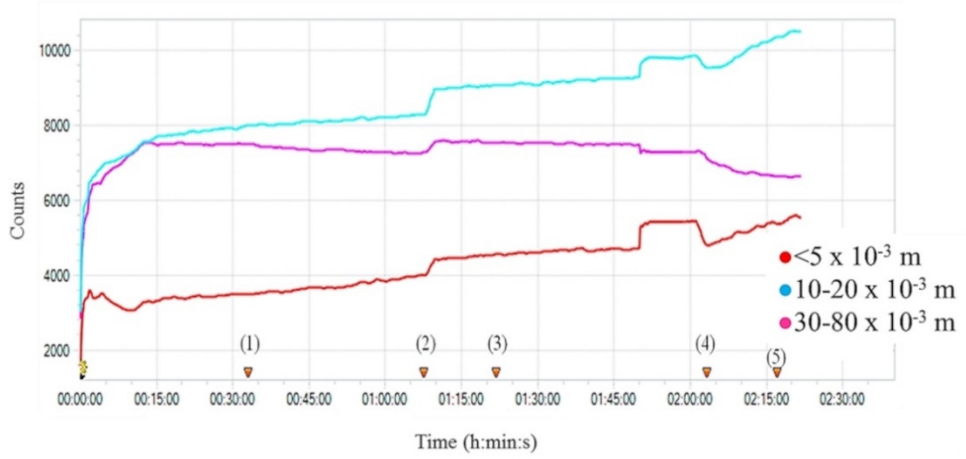

Figure 14. Number of particles as a function of crystallization time: < 5.0 × 10^{-6} (fines), 10–20 × 10^{-6} (fines) and 30–80 × 10^{-6} m. Point (1): setting of agitation velocity (250 rpm) and the beginning of the cooling stage; Point (2): seeding; Point (3): change in agitation velocity to 400 rpm; Point (4): change in agitation velocity to 500 rpm; Point (5): change in agitation velocity to 800 rpm.

Figure 15 (A) shows that particles were already present in the solution saturated with lactose. This suggests the presence of contaminants, which can act as nuclei for primary nucleation, and may act by lowering the solubility of the lactose, causing the formation of lactose nuclei. According to Mimouni et al. (2005), whey proteins in solution constitute local lactose supersaturation spots, creating favourable conditions for nucleation.

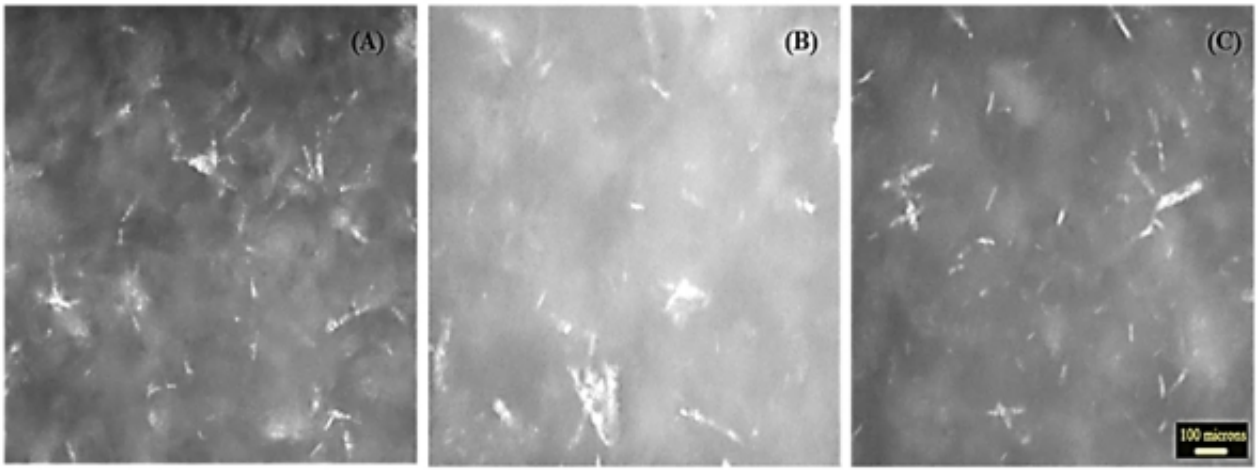

Figure 15. Images of lactose crystals in the crystallization operation in the dilute phase: (A) insertion of solution into the crystallizer; (B) cooling step, T = 60 °C; (C) cooling step, T = 50.0 °C.

Figure 16 shows the images obtained after the seeding stage for the lactose crystallization experiments in the conventional unit and with the dilute phase.

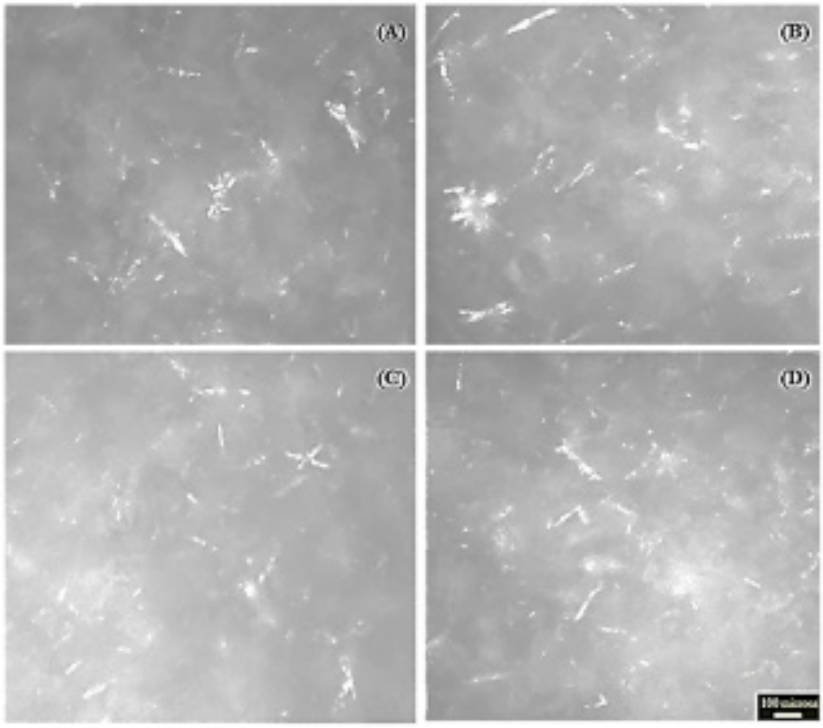

Figure 16. Images of lactose crystals produced in the dilute phase test: (A) 5 min after seeding; (B) 33 min after seed insertion, and 19 min after changing the agitation velocity to 400 rpm; (C) change of agitation velocity to 500 rpm; (D) change of agitation velocity to 800 rpm.

After the seeding stage, a variety of crystalline particles could be observed in solution, from pyramidal to acicular forms, that probably grew before seeding. According to Pisponen et al. (2014), the crystal morphology is more affected by impurities in the solution than by the crystallization conditions. With changes in the agitation rate, there was a tendency to form small particles (fines), probably due to secondary nucleation.

4 Conclusion

Crystallization with in situ and in line monitoring allowed for a more accurate analysis of primary nucleation, growth dynamics, secondary nucleation and microscopy of the crystalline phase in both systems (conventional and vibrated). The vibrating agitation system performed better in terms of particle size distribution, with a smaller population of fines and a crystal population above 30% (30 to 80 μm) as compared to conventional agitation. Operation at low vibration rates allows for an increase in the number of larger particles. The larger crystals tended to fragment when the system was operated at a higher stirring intensity. A greater degree of fragmentation was noted for the purified and concentrated whey. Intensive fines formation was observed in the pre-seeding period for operations using purified whey. Purification of the solution should be intensified in order to obtain better crystal size distribution in the crystallization from whey. The results indicated that crystallization in the vibrated system should be carried out with a vibration frequency of 250 rpm, since increasing it to 400 rpm reduced the amount of larger crystals.

Nomenclature

A_{ex} vibration amplitude (m)

g gravity acceleration (m s^{-2})

r eccentric agitation velocity (rpm)

T temperature (°C)

Γ dimensionless vibration number (-)

ω_{ex} angular vibration frequency (1 s^{-1})

References

Caric, M. (1994). Whey-manufacturing procedures. In M. Caric, *Concentrated and dried dairy products* (pp. 155-162). New York: VCH Publishers, Inc..

De Wit, J. N. (2001). *Lecturer's handbook on whey and whey products* (1a ed.). Brussels, Belgium: European Whey Products Association, 89 p.

Early, R. (1998). Milk concentrates and milk powders. In R. Early, *The technology of dairy products* (pp. 289-290). London, England: Blackie Academic & Professional.

Fedyushkin, A., Bourago, N., Polezhaev, V., & Zharikov, E. (2005). The influence of vibration on hydrodynamics and heat-mass transfer during crystal growth. *Journal of Crystal Growth*, *275*(1-2), 1557-1563. http://dx.doi.org/10.1016/j.jcrysgro.2004.11.220

Finzer, J. R. D., & Malagoni, R. A. (2016). Crystallization. In J. R. D. Finzer & R. A. Malagoni, *Unit operations in the food industry* (pp. 301-347). São Paulo: LTC.

Gernigon, G., Piot, M., Beaucher, E., Jeantet, R., & Schuck, P. (2009). Physicochemical characterization of mozzarella cheese wheys and stretchwaters in comparison with several other sweet wheys. *Journal of Dairy Science*, *92*(11), 5371-5377. PMid:19841197. http://dx.doi.org/10.3168/jds.2009-2359

Jayaprakasha, H. M., Ratel, R. S., & Renner, E. (1995). Optimization of precrystallization process for nonhygroscopic whey powder by using reverse osmosis concentrate. *Japanese Journal of Dairy and Food Science*, *44*(3), A113-A121. http://dx.doi.org/10.11465/milkscience.44.A-113

Kutluay, S., Sahin, O., Ceyhan, A. A., & Izgi, M. S. (2017). Design and optimization of production parameters for boric acid crystals with the crystallization process in an MSMPR crystallizer using FBRM and PVM technologies. *Journal of Crystal Growth*, *467*, 172-180. http://dx.doi.org/10.1016/j.jcrysgro.2017.03.027

Lifran, E. V., Vu, T. T. L., Durham, R. J., Hourigan, J. A., & Sleigh, R. W. (2007). Crystallisation kinetics of lactose in the presence of lactose phosphate. *Powder Technology*, *179*(1-2), 43-54. http://dx.doi.org/10.1016/j.powtec.2006.11.010

Linga, A. (2017). *Effects of seeding on the crystallization behaviour and filtration abilities of an aromatic amine* (Master's Thesis). Department of Chemical Engineering, Norwegian University of Science and Technology, Norway.

Markande, A., Nezzal, A., Fitzpatrick, J., & Redl, A. (2012). Influence of impurities on the crystallization of dextrose monohydrate. *Journal of Crystal Growth*, *353*(1), 145-151. http://dx.doi.org/10.1016/j.jcrysgro.2012.04.021

Mimouni, A., Schuck, P., & Bouhallab, S. (2005). Kinetics of lactose crystallization and crystal size as monitored by refractometry and laser light scattering: effect of proteins. *Le Lait*, *85*(4-5), 253-260. http://dx.doi.org/10.1051/lait:2005015

Modler, H., & Lefkovitch, L. P. (1986). Influence of pH, casein, and whey protein denaturation on the composition, crystal size, and yield of lactose from condensed whey. *Journal of Dairy Science*, *69*(3), 684-697. http://dx.doi.org/10.3168/jds.S0022-0302(86)80457-X

Mullin, J. W. (1988). Crystallization and precipitation. In S. S. Chadwick, *Ullmann's encyclopedia of industrial chemistry* (v. B-2, chap. 3, p. 1-46). Weinheim, Germany: W. Gerhartz.

Narducci, O., Jones, A. G., & Kougoulos, E. (2011). Crystal product engineering in the seeded cooling crystallization of adipic acid from aqueous solution. *Organic Process Research & Development*, *15*(5), 974-980. http://dx.doi.org/10.1021/op200029h

Pakowski, Z., Mujumdar, A. S., & Strumillo, C. (1984). Theory and applications of vibrated beds and vibrated fluid beds for drying processes. In A. S. Mujumdar, *Advances in drying*. Washington: Hemisphere Publishing Co.

Parimaladevi, P., & Srinivasan, K. (2014). Studies on the effect of different operational parameters on the crystallization kinetics of α-lactose monohydrate single crystals in aqueous solution. *Journal of Crystal Growth*, *401*, 252-259. http://dx.doi.org/10.1016/j.jcrysgro.2013.11.015

Pisponen, A., Pajumägi, S., Mootse, H., Sats, A., Poikalainen, V., & Karus, A. (2014). Effect of cooling rates and low crystallization temperatures on morphology of lactose crystals obtained from Ricotta cheese whey. *Agronomy Research (Tartu)*, *12*(3), 787-792.

Shi, Y., Liang, B., & Hartel, R. W. (2006). United States patent US 2006/0128953 A1.

Shin, D. M., & Kim, W. S. (2002). Drowning-out crystallization of L-ornithine-aspartate in turbulent agitated reactor. *Journal of Chemical Engineering of Japan*, *35*(11), 1083-1090. http://dx.doi.org/10.1252/jcej.35.1083

Srisa-nga, S., Flood, A. E., & White, E. T. (2006). The secondary nucleation threshold and crystal growth of r-glucose monohydrate in aqueous solution. *Crystal Growth & Design*, *6*(3), 795-801. http://dx.doi.org/10.1021/cg050432r

Teixeira, G. A. (2014). *Vibrated bed crystallization: purified cheese whey use in lactose separation* (Ph.D. Thesis). School of Chemical Engineering, Federal University of Uberlândia, Uberlândia.

Twieg, W. C., & Nickerson, T. A. (1968). Kinetics of lactose crystallization. *Journal of Dairy Science*, *51*(11), 1720-1724. http://dx.doi.org/10.3168/jds.S0022-0302(68)87265-0

Walstra, P. (2003). Nucleation. In: P. Walstra (Ed.), *Physical chemistry of foods* (pp. 548-582). New York, Marcel Dekker, Inc.

Wong, S. Y., Bund, R. K., Connelly, R. K., & Hartel, R. W. (2011). Determination of the dynamic metastable limit for α-lactose monohydrate crystallization. *International Dairy Journal*, *21*(11), 839-847. http://dx.doi.org/10.1016/j.idairyj.2011.05.003

Wong, S. Y., Bund, R. K., Connelly, R. K., & Hartel, R. W. (2012). Designing a lactose crystallization process based on dynamic metastable limit. *Journal of Food Engineering*, *111*(4), 642-654. http://dx.doi.org/10.1016/j.jfoodeng.2012.03.003

Zadow, J. G. (1984). Lactose: properties and uses. *Journal of Dairy Science*, *67*(11), 2654-2679. http://dx.doi.org/10.3168/jds.S0022-0302(84)81625-2

Funding: CNPq, UFU, Mettler Toledo and Tanac for the support given in the development of this work.

Received: June 19, 2018; Accepted: Apr. 27, 2019